

Accepted Manuscript

In vitro targeting of colon cancer cells using spiropyrazoline oxindoles

Rute C. Nunes, Carlos J.A. Ribeiro, Ângelo Monteiro, Cecília M.P. Rodrigues, Joana D. Amaral, Maria M.M. Santos



PII: S0223-5234(17)30579-2

DOI: [10.1016/j.ejmech.2017.07.057](https://doi.org/10.1016/j.ejmech.2017.07.057)

Reference: EJMECH 9620

To appear in: *European Journal of Medicinal Chemistry*

Received Date: 20 April 2017

Revised Date: 23 June 2017

Accepted Date: 23 July 2017

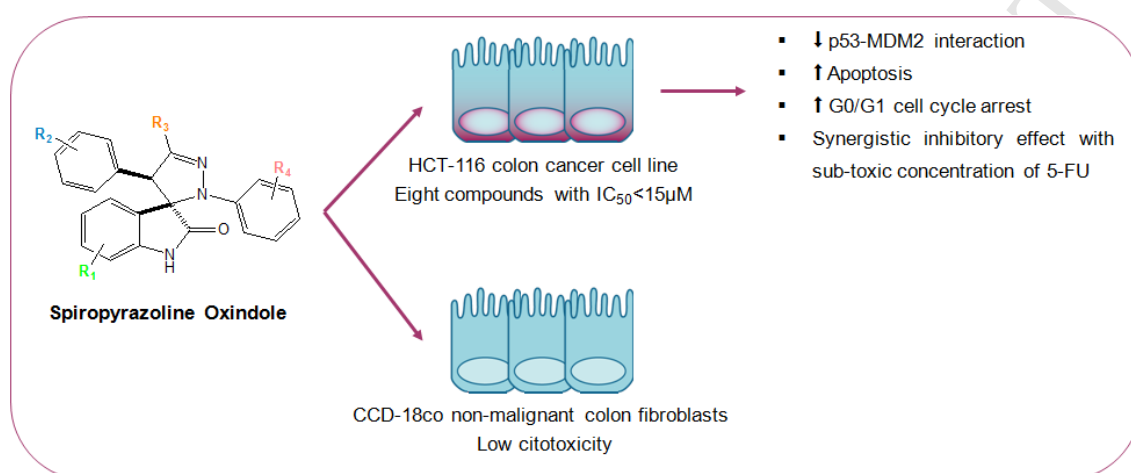
Please cite this article as: R.C. Nunes, C.J.A. Ribeiro, Â. Monteiro, Cecí.M.P. Rodrigues, J.D. Amaral, M.M.M. Santos, *In vitro* targeting of colon cancer cells using spiropyrazoline oxindoles, *European Journal of Medicinal Chemistry* (2017), doi: 10.1016/j.ejmech.2017.07.057.

This is a PDF file of an unedited manuscript that has been accepted for publication. As a service to our customers we are providing this early version of the manuscript. The manuscript will undergo copyediting, typesetting, and review of the resulting proof before it is published in its final form. Please note that during the production process errors may be discovered which could affect the content, and all legal disclaimers that apply to the journal pertain.

In vitro targeting of colon cancer cells using spiropyrazoline oxindoles

Rute C. Nunes, Carlos J. A. Ribeiro, Ângelo Monteiro, Cecília M. P. Rodrigues, Joana D. Amaral*, Maria M. M. Santos*

Research Institute for Medicines (iMed.Ulisboa), Faculty of Pharmacy, Universidade de Lisboa. Av. Prof. Gama Pinto, 1649-003 Lisbon, Portugal



***In vitro* targeting of colon cancer cells using spiropyrazoline oxindoles**

Rute C. Nunes, Carlos J. A. Ribeiro, Ângelo Monteiro, Cecília M. P. Rodrigues, Joana D. Amaral*, Maria M. M. Santos*

Research Institute for Medicines (iMed.Ulisboa), Faculty of Pharmacy, Universidade de Lisboa. Av. Prof. Gama Pinto, 1649-003 Lisbon, Portugal

***Corresponding authors**

Maria M. M. Santos/ Joana D. Amaral

Research Institute for Medicines, iMed.Ulisboa

Faculty of Pharmacy, Universidade de Lisboa

Av. Prof. Gama Pinto, 1649-003 Lisbon, Portugal

Phone: (+) 351 21 794 6400; Fax: (+) 351 21 794 6470

E-mail: mariasantos@ff.ulisboa.pt/ jamaral@ff.ulisboa.pt

Abstract

We report on the synthesis and biological evaluation of a library of twenty-three spiropyrazoline oxindoles. The antiproliferative activity of the chemical library was evaluated in HCT-116 $p53^{(+/+)}$ human colon cancer cell line with eight derivatives displaying good activities ($IC_{50} < 15 \mu M$). To characterize the molecular mechanisms involved in compound antitumoral activity, two spiropyrazoline oxindoles were selected for further studies. Both compounds were able to induce apoptosis and cell cycle arrest at G0/G1 phase and upregulated p53 steady-state levels, while decreasing its main inhibitor MDM2. Importantly, cytotoxic effects induced by spiropyrazolines oxindoles occurred in cancer cells without eliciting cell death in non-malignant CCD-18Co human colon fibroblasts. Additionally, we demonstrated that the combination of spiropyrazoline oxindole **2e** with sub-toxic concentrations of the chemotherapeutic agent 5-fluorouracil (5-FU) exerted a synergistic inhibitory effect on HCT-116 colon cancer cell proliferation. Collectively, our results show the potential of spiropyrazoline oxindoles for development of novel anticancer agents.

Keywords: spirooxindoles; pyrazoline; cytotoxicity; anticancer agents; colorectal cancer.

1. Introduction

Cancer is a multifaceted and multifactorial disease comprised of complex genetic and epigenetic aberrations that destabilize the normal balance of cell homeostasis [1]. Colorectal cancer (CRC) is among the five most diagnosed cancers and it is also the main contributor for mortality and health loss [2,3]. The most often used drugs for CRC include 5-fluorouracil (5-FU), irinotecan, oxaliplatin, and trifluridine combined with tipiracil. Frequently, two or more of these drugs are combined to achieve greater efficacy.

Over the years, several studies have shown the importance of the p53 tumor suppressor protein in cellular homeostasis. This transcription factor is found inactivated in approximately 50% of all human cancers, either by mutation or deletion of its gene, while in the other cases the p53 pathway is partially abrogated by inactivation of other signaling components [4]. The role of p53 is well established in the development of several types of malignant diseases, such as in CRC [3]. In tumors expressing wild-type p53, the inactivation of p53 is frequently observed by reversible inhibition, which results from the overexpression of p53 main negative regulators, MDM2 and MDMX. Several studies have shown that p53 interaction with MDM2 and MDMX involves three main hydrophobic amino acids (Phe₁₉, Trp₂₃ and Leu₂₆) in the p53 protein.

The p53 reactivation can be facilitated by inhibition of its negative regulators. In recent years, several families of compounds have been designed and developed as modulators of p53, such as spirooxindoles compounds [5,6]. This family of compounds is frequently reported as a core structure of a variety of medicinal agents and natural products used in several therapeutic applications, such as in anticancer therapy [7]. However, the development of a p53 reactivating treatment through inhibition of p53–MDM interaction is only just beginning, with few candidates entering in clinical trials (e.g. compound SAR405838) [8]. In this regard, the discovery of more potent and selective small molecule inhibitors of p53–MDM interaction is still an unmet need.

In an attempt to find novel anti-cancer agents, over the last years, we have been developing novel spirooxindoles with different spiro five-membered rings [7,9–11] (Figure 1). More specifically, we have developed a family of spiroisoxazoline oxindoles **1**, in which the most potent derivative showed an IC₅₀ of 26 μM in HCT-116 human colon carcinoma cell line [9]. By changing the isoxazoline oxygen to a *N*-phenyl group,

spiropyrazoline oxindoles **2** were obtained, presenting good antiproliferative activity in human breast cancer cell lines [10]. Here, we report on the synthesis of novel spiropyrazoline oxindole derivatives and the evaluation of biological effects in human colon carcinoma cells.

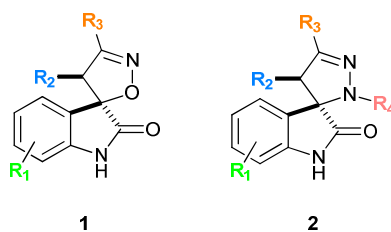
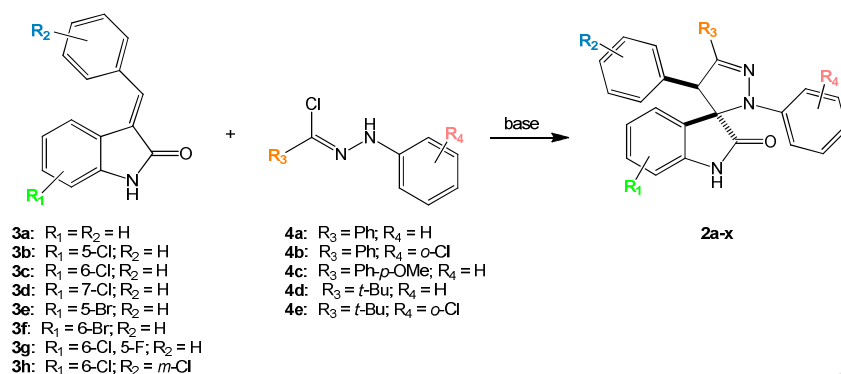


Figure 1 - Spiroisoxazoline oxindoles **1** and spiropyrazoline oxindoles **2** chemical structures.

2. Results and discussion

2.1. Synthesis of a library of spiropyrazoline oxindoles and structure-activity relationship studies (SAR)

Previous studies with spirooxindoles have shown that the presence of a halogen in the oxindole moiety can sometimes increase the antiproliferative activity and the selectivity profile in cancer cell lines [9–13]. Therefore, we have synthesized spiropyrazoline oxindoles with different halogens at the oxindole moiety and different substituents attached to the pyrazoline ring. To validate the importance of having a halogen in the oxindole moiety, derivatives lacking this substituent were also synthesized. Moreover, different substituents in the pyrazoline ring were evaluated, such as aromatic groups (with both electron-withdrawing and electron-donating groups) and the aliphatic group *t*-butyl. Specifically, spiropyrazoline oxindoles **2a-x** were obtained by 1,3-dipolar cycloaddition reaction between 2-indolinones **3** and hydrazonoyl chlorides **4** (Scheme 1). Compounds **3a-h** were synthesized by aldolic condensation reaction of substituted 2-indolinones with different aromatic aldehydes in the presence of piperidine, as reported previously [10,14–17]. Additionally, 2-indolinone **3e** was synthesized by reaction of 5-bromo isatin in the presence of hydrazine monohydrate and ethylene glycerol, under reflux [18]. The relative configuration of the final products was established by NMR comparison with other spiropyrazoline oxindoles described in the literature, with published X-ray crystallography structure [19,20].



Scheme 1 – General scheme for the synthesis of spiro-pyrazoline oxindoles **2a-x**.

The antiproliferative potential of spiro-pyrazoline oxindoles derivatives **2a-x** (Figure 2) was first evaluated in human colon carcinoma HCT-116 cells expressing wild-type p53 (HCT-116 *p53*^(+/+)) to compare the activity of this chemical family with previously developed spirooxindoles, which presented good activities in this cancer cell line [11,21]. The results showed that the most active compounds were **2b**, **2e**, **2g**, **2i**, **2j**, **2l**, **2m** and **2q** (Table 1). The structure-activity relationship studies for this family of compounds indicated that by changing a *tert*-butyl by a *p*-methoxy group at the R₃ group (compound **2s** versus compound **2l**) leads to increased activity in HCT-116 cells. Changing the phenyl group by a *p*-chloro phenyl group, at the R₄ group, in most cases (compound **2v** versus compound **2o** and compound **2d** versus compound **2h**) resulted in decreasing activities, with IC₅₀ values higher than 20 μM. Quite interestingly, spiro-pyrazoline oxindole derivatives **2** were more active than the corresponding spiroisoxazoline oxindoles **1** counterparts. In particular, the presence of a *N*-phenyl group (compounds **2c**, **2f** and **2l**) in the five-membered ring led to an increase in potency, representing a more than 2-fold increase compared to the equivalent spiroisoxazoline oxindoles (compounds **1a**, **1b** and **1c**) (Table 2) [9]. This reassures the importance of including an extra aryl group to improve the activity of the spiro-pyrazoline oxindoles.

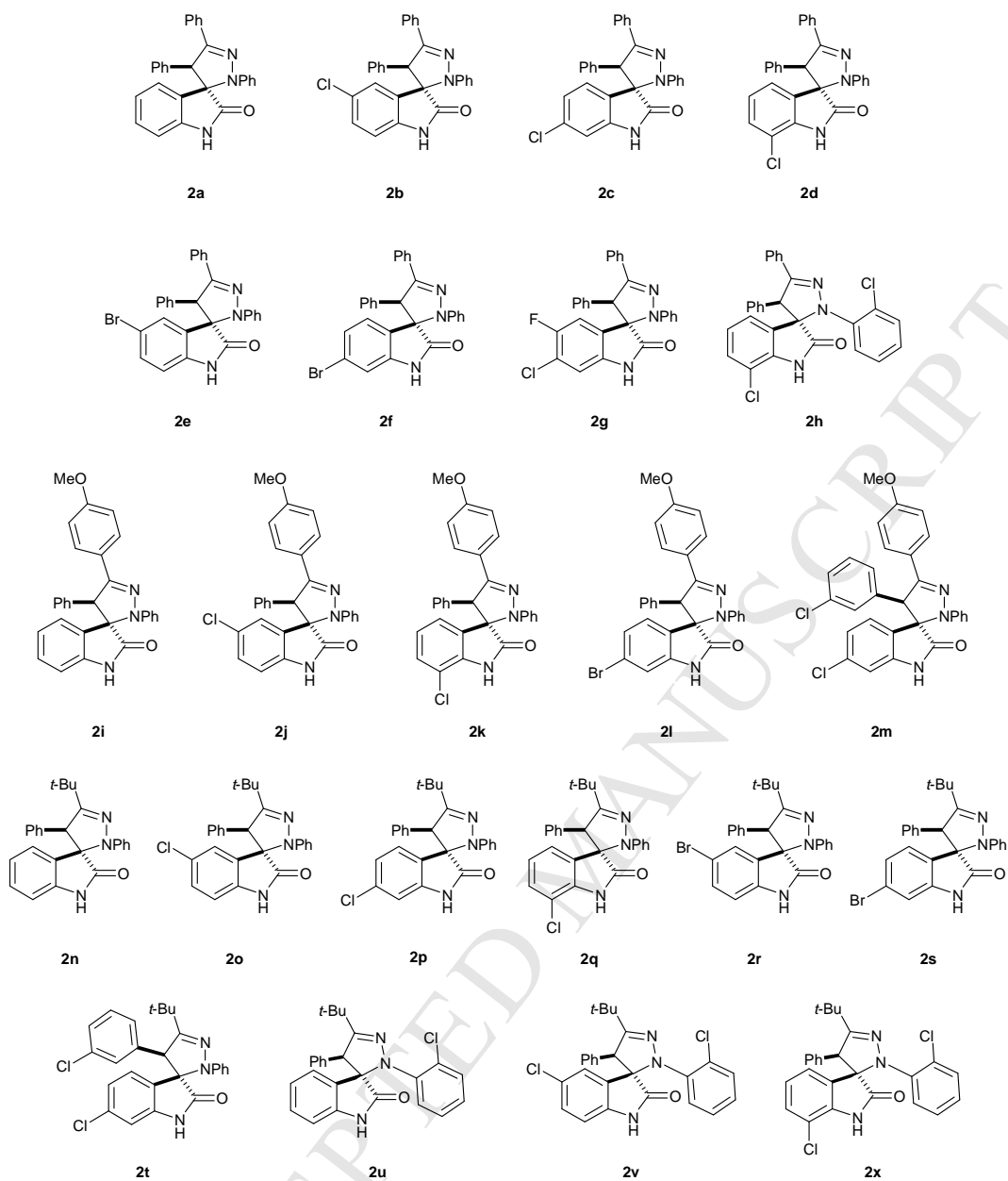


Figure 2 - Spirooxindoles screened in this study.

Table 1 - *In vitro* antiproliferative activities of spiropyrazoline oxindoles **2a-x**.

Compound	R ₁	R ₂	R ₃	R ₄	HCT-116 p53 ^(+/+) IC ₅₀ , μM ^[a]
2a	H	Ph	Ph	Ph	>20
2b	5-Cl	Ph	Ph	Ph	11.0±0.3
2c	6-Cl	Ph	Ph	Ph	16.7±0.9
2d	7-Cl	Ph	Ph	Ph	16.6±1.5
2e	5-Br	Ph	Ph	Ph	13.1±1.0
2f	6-Br	Ph	Ph	Ph	15.9±0.6
2g	6-Cl, 5-F	Ph	Ph	Ph	12.4±0.7
2h	7-Cl	Ph	Ph	Ph- <i>o</i> -Cl	>20
2i	H	Ph	Ph- <i>p</i> -O-CH ₃	Ph	11.7±0.3
2j	5-Cl	Ph	Ph- <i>p</i> -O-CH ₃	Ph	10.6±1.5
2k	7-Cl	Ph	Ph- <i>p</i> -O-CH ₃	Ph	15.6±0.9
2l	6-Br	Ph	Ph- <i>p</i> -O-CH ₃	Ph	12.8±0.7
2m	6-Cl	Ph- <i>m</i> -Cl	Ph- <i>p</i> -O-CH ₃	Ph	10.9±0.8
2n	H	Ph	<i>t</i> -Bu	Ph	>20
2o	5-Cl	Ph	<i>t</i> -Bu	Ph	17.0±1.3
2p	6-Cl	Ph	<i>t</i> -Bu	Ph	>20
2q	7-Cl	Ph	<i>t</i> -Bu	Ph	13.3±1.4
2r	5-Br	Ph	<i>t</i> -Bu	Ph	>20
2s	6-Br	Ph	<i>t</i> -Bu	Ph	>20
2t	6-Cl	Ph- <i>m</i> -Cl	<i>t</i> -Bu	Ph	18.4±1.8
2u	H	Ph	<i>t</i> -Bu	Ph- <i>o</i> -Cl	>20
2v	5-Cl	Ph	<i>t</i> -Bu	Ph- <i>o</i> -Cl	>20
2x	7-Cl	Ph	<i>t</i> -Bu	Ph- <i>o</i> -Cl	17.3±0.2

^[a] IC₅₀ determined by the MTS method after 72 h compound incubation. Each value is the mean (IC₅₀ ± SD) of three independent experiments performed in duplicate.

Table 2 – IC₅₀ values obtained for spiroisoxazoline oxindoles **1** and the corresponding counterparts spiropyrazoline oxindoles **2**.

Compound	R ₁	R ₂	R ₃	R ₄	HCT-116 p53 ^(+/+) IC ₅₀ , μM
2c	6-Cl	Ph	Ph	Ph	16.7±0.9
1a	6-Cl	Ph	Ph	-	39.8±1.1
2f	6-Br	Ph	Ph	Ph	15.9±0.6
1b	6-Br	Ph	Ph	-	35.0±1.1
2l	6-Br	Ph	Ph- <i>p</i> -O-CH ₃	Ph	12.8±0.7
1c	6-Br	Ph	Ph- <i>p</i> -O-CH ₃	-	33.4±1.1

2.2. **2e** and **2m** inhibit p53-MDM2 interaction

To better characterize the molecular mechanisms underlying the antiproliferative activity of this chemical library, we selected two of the active compounds (compounds **2e** and **2m**) for further analysis. Firstly, we investigated if these spirooxindole derivatives could inhibit p53 interaction with its inhibitor MDM2 as described for other five-membered ring spirooxindoles [22,23] (e.g. spirooxindole MI-77301). For that, we used a simple assay that allows the direct visualization and quantification of p53-MDM2 interaction in live cells [9,24]. The system relies on a Venus-based bimolecular fluorescence complementation (BiFC) assay, where p53 and MDM2 are fused to non-fluorescent fragments of Venus fluorescent reporter protein (V1 and V2). When both proteins interact, the non-fluorescent halves get close enough to fold together and reconstitute the functional fluorophore. Fluorescence is therefore proportional to the amount of p53-MDM2 dimers generated, and can be analyzed by flow cytometry. As shown in Figure 3, exposure of HCT-116 $p53^{(-/-)}$ cells co-transfected with V1-p53 and MDM2-V2 to compounds **2e** and **2m** at 20 μ M concentration resulted in a mild but significant decrease of BiFC signal ($p < 0.05$) corresponding to disruption of the p53-MDM2 interaction. We obtained similar results when using nutlin-3a at half the concentration as positive control.

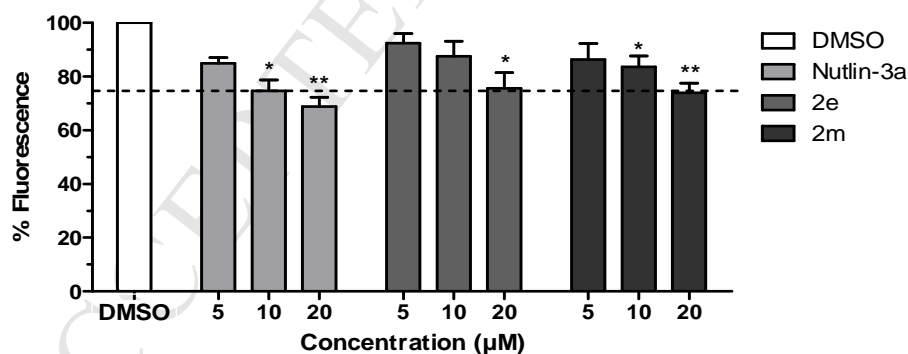


Figure 3 - Compounds **2e** and **2m** inhibit p53-MDM2 interaction. HCT-116 $p53^{(-/-)}$ cells were co-transfected with the V1-p53/MDM2-V2 BiFC constructs for 24 h. Vehicle, nutlin-3a and compounds **2e** and **2m** were included in the culture medium 4 h after transfection. V1-p53/MDM2-V2 complementation was evaluated by flow cytometry. Results are expressed as the percentage (%) of fluorescence normalized to vehicle control DMSO (100% fluorescence intensity). Data are mean \pm SD of three independent experiments. * $p < 0.05$ and ** $p < 0.01$ versus DMSO control.

Next, the evaluation of the steady-state levels of p53 and MDM2 was made by Western blot. As depicted in Figure 4, incubation of HCT-116 $p53^{+/+}$ cells with compounds **2e** and **2m** at the IC_{50} concentration induced slight variations in p53 and MDM2 total levels, with a tendency to increase p53 and decrease MDM2 levels.

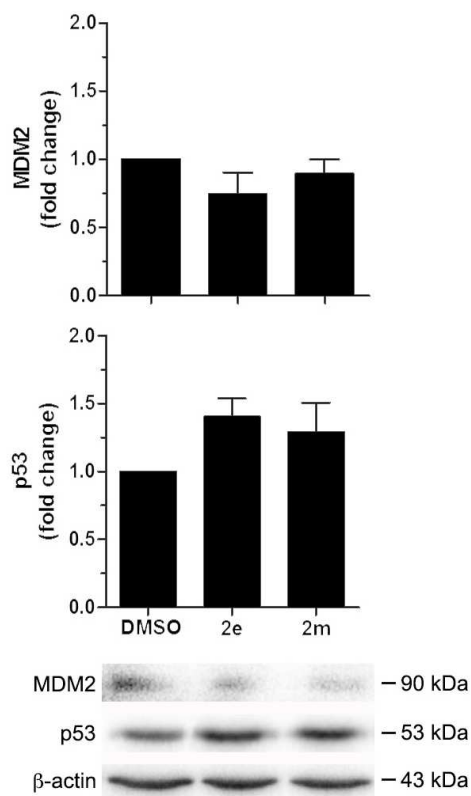


Figure 4 – Effect of compounds **2e** and **2m** in p53 and MDM2 protein levels. Total proteins were isolated from HCT-116 $p53^{+/+}$ cells following incubation with compounds **2e** and **2m** at IC_{50} concentration, or DMSO (vehicle control), for 72 h. Blots were normalized to endogenous β -actin. Data represent mean \pm SEM of two independent experiments.

To confirm the contribution of p53 activation to compound activity in HCT-116 $p53^{+/+}$ cells, **2e** and **2m** were tested in HCT-116 cells in which p53 has been knocked out (HCT-116 $p53^{-/-}$). None of the compounds was selective for HCT-116 $p53^{+/+}$ over HCT-116 $p53^{-/-}$ cells (**2e** IC_{50} =14.2 \pm 0.8 μ M; **2m** IC_{50} =11.6 \pm 0.8 μ M), revealing that other mechanisms, besides p53-dependent effects, may contribute for compounds antiproliferative activity. This result was further supported by evaluating the binding of spiropyrazoline oxindole **2e** with MDM2 using a fluorescence polarization (FP) competitive binding assay. Compound **2e** was not able to compete with the fluorescent

probe molecule, which binds to MDM2 potently, up to 400 μM . This contrasts with the reported MDM2 inhibitor Nutlin-3a developed by Roche.

2.3. **2e** and **2m** induce cell death and cell cycle arrest

The levels of general cell death were evaluated by measuring the enzymatic activity of lactate dehydrogenase (LDH) released from damaged cells. Surprisingly, the results revealed that incubation of HCT-116 $p53^{+/+}$ cells with compounds **2e** and **2m** at the IC_{50} concentration for 72 hours, did not induce the release of LDH (Figure 5). However, when both compounds were used at twice of the IC_{50} concentration the LDH activity was approximately 1.5-fold higher comparing to DMSO controls, suggesting that membrane permeabilization and leakage of cytosolic cellular contents, such as LDH, may be a late-stage event in the cell death cascade. In contrast, mitochondria dysfunction, an organelle partially involved in MTS metabolism, may represent an initial event.

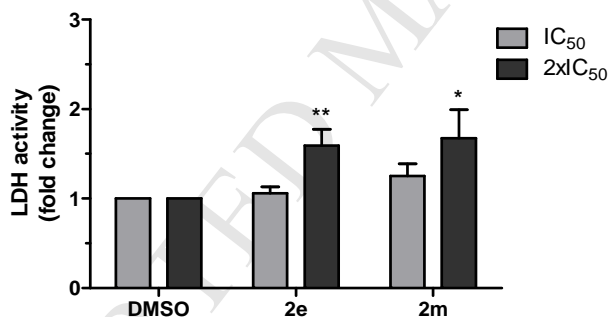


Figure 5 - Compounds **2e** and **2m** induce cell death in HCT-116 $p53^{+/+}$ cells. General cell death was evaluated by the LDH release assay following 72 h of incubation with compounds **2e** and **2m** at equitoxic (IC_{50} and $2\times\text{IC}_{50}$) concentration, or DMSO (vehicle control). Data are mean \pm SEM of three independent experiments. * $p < 0.05$, ** $p < 0.01$ versus respective DMSO control.

The cell death by apoptosis was assessed by performing a double staining method with Annexin V-FITC and 7-Aminoactinomycin D (7-AAD) followed by flow cytometry analysis. As illustrated in Figure 6, exposure of HCT-116 $p53^{+/+}$ cells to compounds **2e** and **2m** at the IC_{50} concentration, resulted in the induction of apoptosis, as revealed by a 10% increase of cells undergoing early phases of apoptosis. When cells were exposed to the same compounds at twice of the IC_{50} concentration, the percentage

of cells in early apoptosis increased, especially with compound **2m**. Moreover, a massive increase in cells undergoing secondary apoptosis was detected. Since, cell death by apoptosis appears to contribute only in part to compound cytotoxic effects, the association between **2e** and **2m**-induced growth inhibition and the regulation of cell cycle progression was explored. HCT-116 $p53^{+/+}$ cells exposed to compounds **2e** and **2m** at the respective IC_{50} concentrations were collected and stained with propidium iodide (PI) to determine cellular DNA content by flow cytometry. The percentage of cells in each phase of the cell cycle was analyzed after 24 and 48 hours of compound incubation. As observed in Figure 7, compound **2m** induced a significant accumulation of cells in the G0/G1 phase after 24 h, with a concomitant decrease in the G2/M phase, comparing to control ($p < 0.01$). In respect to the S phase, no significant changes were observed.

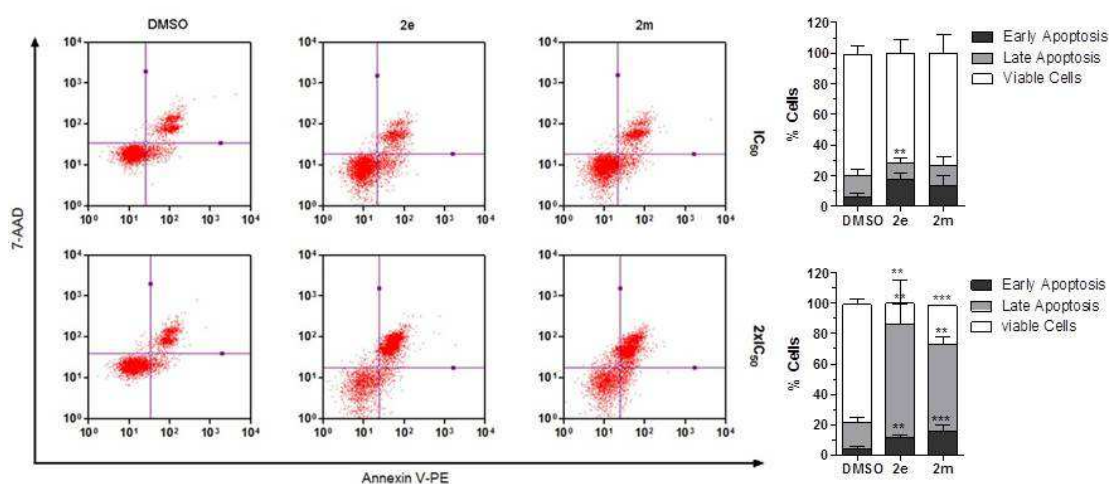


Figure 6 – Compounds **2e** and **2m** induce apoptosis in HCT-116 $p53^{+/+}$. Evaluation of apoptosis by flow cytometry using Guava Nexin assay, following cell incubation with **2e** and **2m** at equitoxic concentrations (IC_{50} and $2xIC_{50}$), or DMSO (vehicle control), for 72 h. Representative flow cytometry profiles (left) and respective quantification (right). Data are mean \pm SD of three independent experiments. ** $p < 0.01$; *** $p < 0.001$ versus DMSO control.

When analysing the DNA content after 48 hours of compound exposure (Figure 7), we observed that treatment with **2e** resulted in accumulation of cells in the G0/G1 phase, representing a total of 62% compared to 42% of cells in the control. Compound **2e** also had an impact in the G2/M phase with a 3-fold reduction in the percentage of cells ($p < 0.01$). Collectively, these data indicate that compounds **2e** and **2m** induce cell cycle arrest in G0/G1 in a time-dependent manner, with **2m** acting earlier than **2e**. The

arrest of cells in the G0/G1 phase may allow the repair of damaged DNA, and/or inhibit cell growth [25,26]. These results suggest that both induction of apoptosis and cell cycle arrest are important mechanisms underlying **2e** and **2m** cytotoxic effects in HCT-116 $p53^{+/+}$ cells.

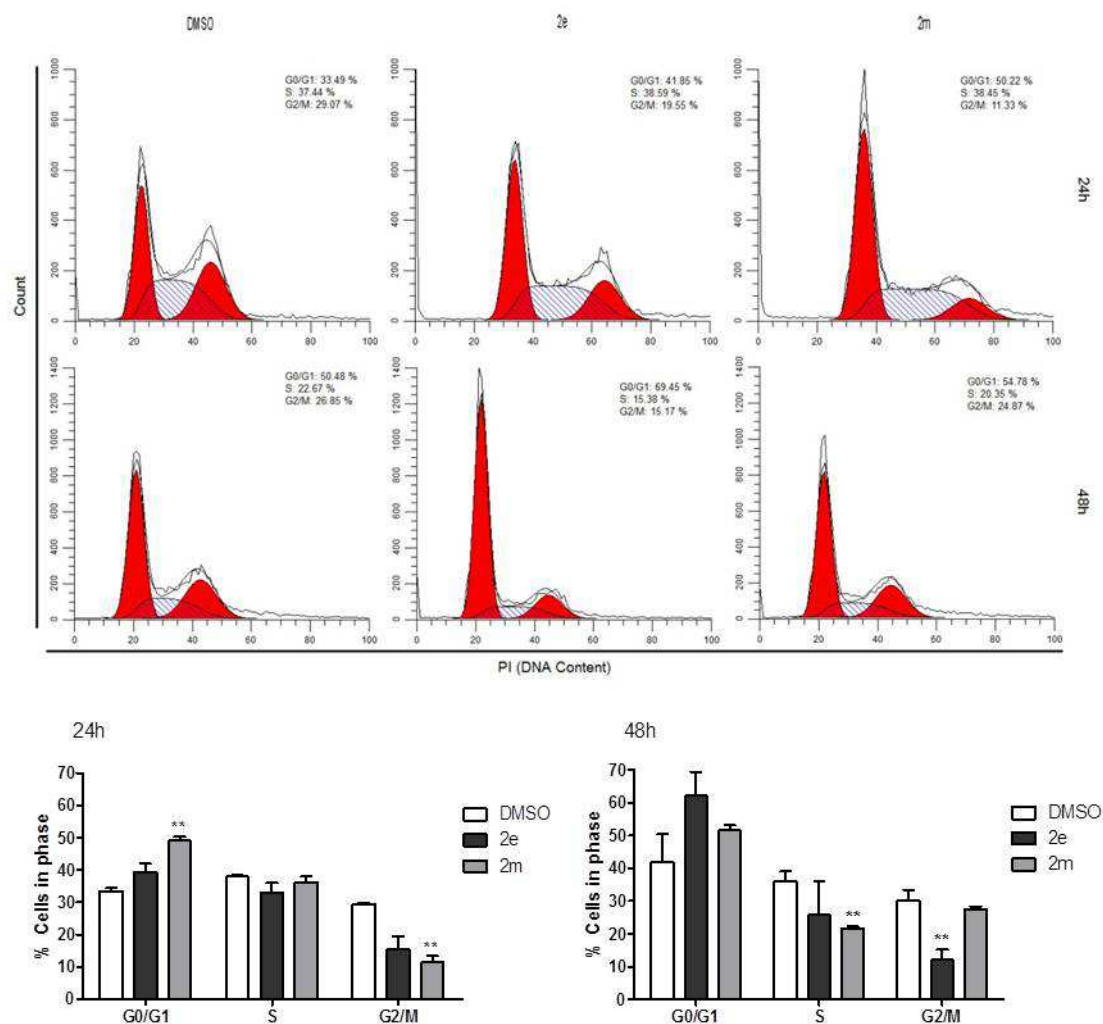


Figure 7 - Effects of compounds **2e** and **2m** on cell cycle progression. HCT-116 $p53^{+/+}$ were treated with compounds **2e** and **2m** at equitoxic (IC_{50}) concentration, or DMSO (vehicle control) for 24 h and 48 h. Cellular DNA was stained with PI, and flow cytometry analysis was performed to determine cell cycle distribution. Following flow cytometry analysis, frequencies of cells in each phase of the cell cycle were calculated using Mod Fit LT 4.1 software. Histograms show one representative example from three independent experiments (top). Results are expressed in the graph bar as means \pm SD of three independent experiments (bottom). ** $p < 0.01$ versus DMSO control.

2.4. **2e** and **2m** are not toxic in human normal colon fibroblasts

Finally, compound cytotoxicity was evaluated in CCD-18Co fibroblasts, a human normal colon cell line. Notably, exposure of CCD-18Co cells to compounds **2e** and **2m** at IC₅₀ concentration (previously determined for HCT-116 *p53*^(+/+)) did not affect viability (Figure 8). When compounds were incubated at IC₈₀ concentration, cell viability decreased in approximately 20%, suggesting that these molecules may serve as promising molecules for further optimization and development of new anti-tumoral agents with reduced off-target effects.

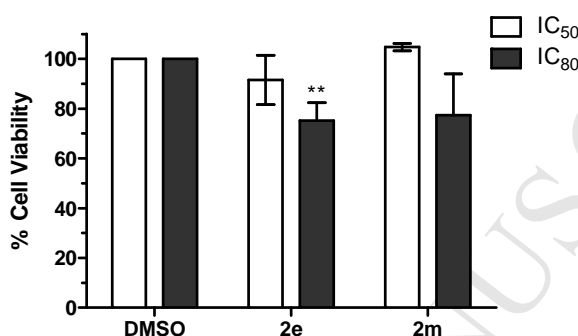


Figure 8- Effect of compounds **2e** and **2m** in a non-tumoral cell line. CCD-18Co human normal colon fibroblasts were incubated with compounds **2e** and **2m** at equitoxic (IC₅₀ and IC₈₀) concentrations as determined for HCT-116 *p53*^(+/+) cells, or vehicle (DMSO), for 72 h. Cell viability was assessed using the MTS metabolism assay. Data are mean \pm SEM of three independent experiments. ***p*<0.01 versus DMSO control.

2.5. Synergistic antiproliferative effect of compound **2e** and 5-fluorouracil

Drug combination is widely used to achieve treatment efficacy of several types of tumors. The main goal is to achieve a synergistic therapeutic effect accompanied by a decrease of toxicity, and diminished drug resistance [27,28]. Taking this into account, we analysed the potential of compound **2e** to increase HCT-116 *p53*^(+/+) cell sensitivity to conventional chemotherapeutic 5-fluorouracil. 5-FU acts as a thymidylate synthase inhibitor (blocking DNA replication) [29,30], while the compounds in test are capable of inducing apoptosis and cell cycle arrest. First, we determined the IC₅₀ value of 5-FU in HCT-116 *p53*^(+/+) cells under the same conditions as we did for compounds in test (data not shown). After that, cells were exposed to a fixed concentration of 5-FU combined with increasing concentrations of compound **2e**. Interestingly, combination of 5-FU at IC₁₀ concentration with **2e** at IC₂₀ concentration resulted in the highest

synergistic effect ($CDI < 1$) (Figure 9). When compound **2e** was used at IC_{10} concentration, a mild synergism was still observed, but the effect was lost when used at IC_{50} concentration ($CDI > 1$) (Figure 9). Overall, the results suggest that combining 5-FU at IC_{10} concentration and compound **2e** at concentrations below the IC_{50} lead to better results and possibly less side effects.

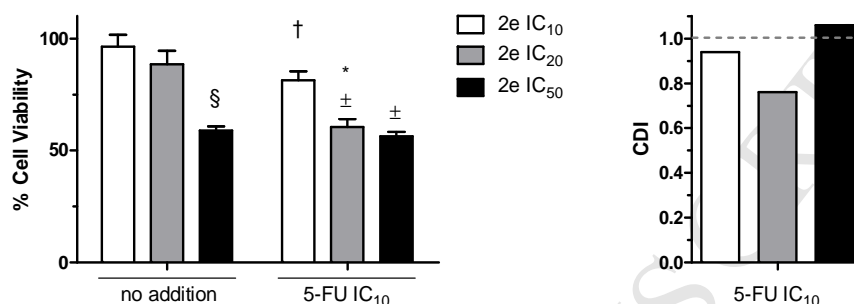


Figure 9 - Coefficient drug interaction (CDI) analysis of compound **2e** with 5-fluorouracil (5-FU). HCT-116 cells were exposed to compounds for 72h and cell viability was evaluated using the MTS metabolism assay. CDI value threshold = 1. **2e** [IC_{10}]=9.5 μ M; **2e** [IC_{20}]=10.7 μ M; **2e** [IC_{50}]=13.0 μ M and **5-FU** [IC_{10}]=1.7 μ M. Data are mean \pm SEM of five independent experiments. $\S p < 0.005$ versus **2e** IC_{10} ; $\dagger p < 0.05$ versus **2e** alone; $* p < 0.01$ versus **2e** alone; $\pm p < 0.005$ versus respective **2e** IC_{10} .

3. Conclusions

A library of twenty-three spiropyrazoline oxindoles was designed and synthesized by 1,3-dipolar cycloaddition reaction. The compounds were screened for the first time in HCT-116 human colon carcinoma cells expressing wild-type p53 and eight spiropyrazoline oxindoles (compounds **2b**, **2e**, **2g**, **2i**, **2j**, **2l**, **2m** and **2q**) displayed activities below 15 μ M. From these, two derivatives were selected to further characterize the molecular mechanisms involved in compound cytotoxicity. Importantly, a dose dependent increase of general cell death and apoptosis was found in HCT-116 cells after treatment with compounds **2e** and **2m**. These compounds also induced time-dependent arrest of cells in G0/G1 phase of cell cycle. Interestingly, compounds **2e** and **2m** showed to partially inhibit p53-MDM2 protein-protein interaction in live cells using a bimolecular fluorescence complementation (BiFC) assay. However, evaluation of these compounds in HCT-116 cells lacking p53 revealed that spiropyrazoline oxindoles activity also rely on other pathways independent from p53 and MDM2. Finally, compounds **2e** and **2m** were non-cytotoxic to human normal

colon fibroblasts for the tested concentrations. Interestingly, combined therapy studies demonstrated a synergistic effect of spiropyrazoline oxindoles with the chemotherapeutic agent 5-FU, which further highlights the potential of this chemical family as anticancer agents.

4. Experimental Section

4.1. Chemistry: General conditions

All chemical and solvents were obtained from commercial suppliers and were used without further purification. When used as reaction solvents, CH₂Cl₂ was dried over CaCl₂ and distilled; THF was distilled from sodiumbenzophenone system. Et₃N was dried over KOH, distilled and stored with molecular sieves. Compounds **2a-2f**, **2j-2l**, **2p**, **2q** and **2s** were synthesized according to the method described in the literature [10]. Compounds **4b**, **4d**, **4e** were synthesized according to the method described in the literature [31] and compounds **4a**, **4c** were synthesized as described in the literature [32,33].

Thin layer chromatography was performed using Merck Silica Gel 60 F254 aluminium plates and visualized by UV light. Flash column chromatography was performed on Merck Silica Gel (200-400 mesh ASTM). Preparative TLC was performed on Merck Silica Gel 60 GF254 over glass plates. ¹H and ¹³C NMR spectra were recorded on a Bruker 400 Ultra-Shield at 400 MHz (¹H NMR) and 101 MHz (¹³C NMR) or on a Bruker 300 Ultra-Shield at 300 MHz (¹H NMR) and 75 MHz (¹³C NMR). ¹H and ¹³C chemical shifts (δ) are expressed in parts per million (ppm) using the solvent as internal reference, and proton coupling constants (J) in hertz (Hz). ¹H spectral data are reported as follows: chemical shift, multiplicity (s, singlet; d, doublet; t, triplet; q, quartet; m, multiplet; dd, doublet of doublets; dt, doublet of triplets, and br, broadened), coupling constant, and integration. The infrared spectra were collected on a Shimadzu FTIR Affinity-1 spectrophotometer. The spectra were determined using KBr disks. Only the most significant absorption bands are reported. All compounds tested showed appropriate purity by elemental analysis (C, H, and N), performed in a Flash 2000 CHNS-O analyzer (ThermoScientific, UK) at Liquid Chromatography and Mass Spectrometry Laboratory, Faculty of Pharmacy of Universidade de Lisboa.

4.1.1. General Procedure for the Synthesis of 2-Indolinones

A reaction mixture of the proper substituted indolin-2-ones **6**, aldehyde (1.2 eq.), and piperidine (0.1 eq.) in ethanol (1 mL/0.5 mmol oxindole) was refluxed for 3-5 h, under nitrogen atmosphere. After, the mixture was cooled and put on ice, where the product precipitated. The product was filtered in vacuum with cold ethanol [10,14–17]. Finally, the product was placed in the vacuum desiccators to give the expected compound. The indolin-2-ones **3e** was generated through substituted isatin in the presence of hydrazine monohydrate and ethylene glycerol, under reflux [18].

4.1.2. General Procedure for the Synthesis of 2',4'-Dihydrospiro[Indoline-3,3'-[Pyrazol]-2-ones(2)

Triethylamine/*N,N*-Diisopropylethylamine was added dropwise to a mixture of indolin-2-one **3** derivative and hydrazonyl chloride **4** derivative in dry CH₂Cl₂ under nitrogen atmosphere. The reaction mixture was quenched with water (H₂O). The phases were separated and the aqueous phase was extracted with Ethyl Acetate (3xEtOAc). The combined organic extracts were dried over anhydrous Na₂SO₄ and the product was dried on the rotary evaporator. The residue was purified by flash chromatography on silica to afford the final spiropyrazoline oxindole compound **2** [10].

6-chloro-5-fluoro-2',4',5'-triphenyl-2',4'-dihydrospiro[indoline-3,3'-pyrazol]-2-one (2g). Following the general procedure, to a solution of **3g** (0.0175 g, 0.06 mmol, 1 eq) in CH₂Cl₂ (2 ml) was added **4a** (0.04 g, 0.16 mmol, 2.5 eq) and triethylamine (0.023 ml, 0.15 mmol, 2.5 eq). Reaction time: 46 h. The compound was purified by flash chromatography (eluent: EtOAc/*n*-Hexane 1:3) to afford compound **2g** as a white solid (0.01 g, 0.03 mmol, 40.0 %); IR (KBr): 3419 (NH), 1730 (C=O), 1597 (C=N) cm⁻¹; ¹H NMR (300 MHz, CDCl₃) δ 8.03 (s, 1H, NH), 7.70-7.60 (m, 2H, ArH), 7.35 – 7.05 (m, 8H, ArH), 7.00 – 6.80 (m, 6H, ArH), 6.17 (d, *J* = 8.0 Hz, 1H, ArH), 5.14 (s, 1H, H-5'); ¹³C NMR (75 MHz, CDCl₃) δ 178.47 (C=O), 154.21 (d, *J* = 243.0 Hz), 149.23 (C=N), 144.07 (Cq), 136.44 (Cq), 133.97 (CH), 131.37 (Cq), 129.26 (CH), 129.16 (CH), 129.06 (CH), 128.69 (CH), 128.62 (CH), 126.99 (CH), 125.80 (d, *J* = 7.2 Hz), 122.09 (d, *J* = 19.5 Hz), 121.69 (CH), 115.48 (CH), 115.17 (d, *J* = 25.5 Hz), 112.52 (CH), 77.00

(Cspiro), 62.81 (CH-5'); LC-MS m/z calcd for $C_{28}H_{19}ClFN_3O$: 467.1, Found: 468.3 $[M^+H]^+$.

7-chloro-2'-(2-chlorophenyl)-4',5'-diphenyl-2',4'-dihydrospiro[indoline-3,3'-pyrazol]-2-one (2h). Following the general procedure, to a solution of **3d** (0.05 g, 0.20 mmol, 1 eq) in CH_2Cl_2 (1.5 ml) was added **4b** (0.08 g, 0.29 mmol, 1.5 eq) and *N,N*-Diisopropylethylamine (0.10 mL, 0.59 mmol, 3 eq.). Reaction time: 23 h. The compound was purified by flash chromatography (eluent: EtOAc/*n*-Hexane 1:4) to afford compound **2h** as a white solid (0.09 g, 0.18 mmol, 93.9 %); IR (KBr): 3412 (NH), 1720 (C=O), 1620 (C=N) cm^{-1} ; 1H NMR (300 MHz, $CDCl_3$) δ 7.79 (s, 1H, NH), 7.71 – 7.63 (m, 2H, ArH), 7.44 (dd, $J = 8.4, 1.3$ Hz, 1H, ArH), 7.30-7.25 (m, 3H, ArH), 7.23 – 7.13 (m, 5H, ArH), 7.10 – 6.95 (m, 4H, ArH), 6.34 (t, $J = 7.9$ Hz, 1H, ArH), 5.89 (d, $J = 7.5$ Hz, 1H, ArH), 5.07 (s, 1H, H-5'); ^{13}C NMR (75 MHz, $CDCl_3$) δ 177.61 (C=O), 151.84 (C=N), 141.18 (Cq), 138.50 (Cq), 134.80 (Cq), 131.51 (Cq), 130.37 (CH), 129.72 (Cq), 129.22 (CH), 129.11 (CH), 128.95 (CH), 128.55 (CH), 128.24 (CH), 127.27 (CH), 127.12 (CH), 126.55 (CH), 126.00 (CH), 125.88 (CH), 125.50 (Cq), 122.42 (CH), 114.65 (Cq), 78.98 (Cspiro), 62.59 (CH-5'); Anal. Calc. for $C_{28}H_{19}Cl_2N_3O$: C 69.42, H 3.96, N 8.68, Found: C 69.04, H 3.78, N 9.30.

5'-(4-methoxyphenyl)-2',4'-diphenyl-2',4'-dihydrospiro[indoline-3,3'-pyrazol]-2-one (2i). Following the general procedure, to a solution of **3a** (0.075 g, 0.34 mmol, 1 eq) in CH_2Cl_2 (2 ml) was added **4c** (0.13 g, 0.51 mmol, 1.5 eq) and triethylamine (0.14 ml, 1.02 mmol, 3 eq). Reaction time: 17 h. The compound was purified by flash chromatography (eluent: EtOAc/*n*-Hexane 1:3) to afford compound **2i** as a white solid (0.1 g, 0.3 mmol, 73.5 %); IR (KBr): 3362 (NH), 1741 (C=O), 1600 (C=N) cm^{-1} ; 1H NMR (400 MHz, $CDCl_3$) δ 8.63 (s, 1H, NH), 7.62 (d, $J = 8.0$ Hz, 2H, ArH), 7.16 – 7.00 (m, 6H, ArH), 7.00-6.90 (m, 4H, ArH), 6.85-6.78 (m, 3H, ArH), 6.74 (d, $J = 8.0$ Hz, 1H, ArH), 6.57 (t, $J = 8.0$ Hz, 1H, ArH), 6.36 (d, $J = 8.0$ Hz, 1H, ArH), 5.13 (s, 1H, H-4'), 3.78 (s, 3H, CH_3); ^{13}C NMR (101 MHz, $CDCl_3$) δ 178.52 (C=O), 160.08 (C=N), 148.81 (Cq), 144.48 (Cq), 139.89 (Cq), 134.75 (Cq), 129.31 (CH), 129.21 (CH), 128.91 (CH), 128.53 (CH), 128.36 (CH), 127.88 (CH), 126.47 (CH), 125.72 (Cq), 124.41 (Cq), 122.36 (CH), 120.78 (CH), 115.25 (CH), 113.86 (CH), 110.44 (CH), 77.23 (Cspiro), 62.78 (CH-4'), 55.26 (O- CH_3); Anal. Calc. for $C_{29}H_{23}N_3O_2$: C 78.18, H 5.20, N 9.43, Found: C 77.96, H 5.19, N 9.34.

6-chloro-4'-(3-chlorophenyl)-5'-(4-methoxyphenyl)-2'-phenyl-2',4'-

dihydrospiro[indoline-3,3'-pyrazol]-2-one (2m). Following the general procedure, to a solution of **3h** (0.075 g, 0.26 mmol, 1 eq) in CH₂Cl₂ (2 ml) was added **4c** (0.14 g, 0.52 mmol, 2 eq) and triethylamine (0.11 ml, 0.78 mmol, 3 eq). Reaction time: 22 h. The compound was purified by flash chromatography (eluent: EtOAc/*n*-Hexane 1:3) and then recrystallized in diethyl ether to afford compound **2m** as a white solid (0.13 g, 0.25 mmol, 97.8 %); IR (KBr): 3406 (NH), 1703 (C=O), 1597 (C=N) cm⁻¹; ¹H NMR (400 MHz, CDCl₃) δ 8.81 (s, 1H, NH), 7.59 (d, *J* = 8.8 Hz, 2H, ArH), 7.17 (d, *J* = 8.0 Hz, 1H, ArH), 7.11 (t, *J* = 8.0 Hz, 3H, ArH), 6.97 (s, 1H, ArH), 6.90 (d, *J* = 8.0 Hz, 2H, ArH), 6.87-6.80 (m, 4H, ArH), 6.78 (d, *J* = 1.5 Hz, 1H, ArH), 6.62 (dd, *J* = 8.0, 1.7 Hz, 1H, ArH), 6.28 (d, *J* = 8.0 Hz, 1H, ArH), 5.02 (s, 1H, H-4'), 3.79 (s, 3H, CH₃); ¹³C NMR (101 MHz, CDCl₃) δ 178.29 (C=O), 160.49 (C=N), 148.59 (Cq), 144.34 (Cq), 141.13 (Cq), 136.73 (Cq), 135.65 (Cq), 134.87 (Cq), 130.18 (CH), 129.18 (CH), 128.58 (CH), 128.46 (CH), 127.48 (Cq), 127.29 (CH), 123.88 (Cq), 122.77 (CH), 121.51 (CH), 115.59 (CH), 114.17 (CH), 111.62 (CH), 76.66 (Cspiro), 62.20 (CH-4'), 55.43 (O-CH₃); Anal. Calcd for C₂₉H₂₁Cl₂N₃O₂: C 67.71, H 4.11, N 8.17, Found: C 67.19, H 4.15, N 7.98.

5'-(tert-butyl)-2',4'-diphenyl-2',4'-dihydrospiro[indoline-3,3'-pyrazol]-2-one (2n).

Following the general procedure, to a solution of **3a** (0.05 g, 0.26 mmol, 1 eq) in CH₂Cl₂ (2 ml) was added **4d** (0.1 g, 0.47 mmol, 2 eq) and triethylamine (0.11 ml, 0.78 mmol, 3 eq). Reaction time: 5h30min. The compound was purified by flash chromatography (eluent: EtOAc/*n*-Hexane 1:3) and then recrystallized in dichloromethane:*n*-hexane to afford compound **2n** as a white solid (0.07 g, 0.16 mmol, 72.7 %); IR (KBr): 3236 (NH), 1709 (C=O), 1599 (C=N) cm⁻¹; ¹H NMR (300 MHz, CDCl₃) δ 7.65 (s, 1H, NH), 7.35 (m, 2H, ArH), 7.16 -6.99 (m, 5H, ArH), 6.83 (dd, *J* = 8.8, 1.0 Hz, 3H, ArH), 6.80 – 6.74 (m, 2H, ArH), 6.57 (td, *J* = 7.6, 1.0 Hz, 1H, ArH), 6.24 (d, *J* = 7.2 Hz, 1H, ArH), 4.46 (s, 1H, H-4'), 1.19 (s, 9H, C(CH₃)₃); ¹³C NMR (75 MHz, CDCl₃) δ 178.37 (C=O), 161.70 (C=N), 145.79 (Cq), 140.40 (Cq), 135.29 (Cq), 129.28 (CH), 128.90 (CH), 128.12 (CH), 126.41 (CH), 125.74 (Cq), 122.24 (CH), 120.92 (CH), 115.96 (CH), 110.46 (CH), 77.28 (Cspiro), 62.32 (CH-4'), 34.87 (C(CH₃)₃), 29.49 (C(CH₃)₃); Anal. Calc. for C₂₆H₂₅N₃O.0.05H₂O: C 78.77, H 6.40, N 10.60, Found: C 77.70, H 6.47, N 10.18.

5'-(tert-butyl)-5-chloro-2',4'-diphenyl-2',4'-dihydrospiro[indoline-3,3'-pyrazol]-2-one (2o). Following the general procedure, to a solution of **3b** (0.05 g, 0.23 mmol, 1 eq) in CH₂Cl₂ (2 ml) was added **4d** (0.09 g, 0.47 mmol, 2 eq) and triethylamine (0.09 ml, 0.68 mmol, 3 eq). Reaction time: 4h50min. The compound was purified by flash chromatography (eluent: EtOAc/*n*-Hexane 1:2) to afford compound **2o** as a white solid (0.08 g, 0.19 mmol, 80.2 %); IR (KBr): 3254 (NH), 1718 (C=O), 1691 (C=N) cm⁻¹; ¹H NMR (300 MHz, CDCl₃) δ 7.62 (s, 1H, NH), 7.47 – 7.34 (m, 2H, ArH), 7.31 (d, *J* = 7.8 Hz, 1H, ArH), 7.20 (m, 1H, ArH), 7.12 – 7.02 (m, 3H, ArH), 6.85-6.78 (m, 4H, ArH), 6.69 (d, *J* = 8.3 Hz, 1H, ArH), 6.15 (d, *J* = 2.1 Hz, 1H, ArH), 4.46 (s, 1H, H-4'), 1.19 (s, 9H, C(CH₃)₃); ¹³C NMR (75 MHz, CDCl₃) δ 177.60 (C=O), 161.51 (C=N), 145.42 (Cq), 138.52 (Cq), 134.53 (Cq), 129.09 (CH), 128.87 (CH), 128.39 (CH), 127.71 (Cq), 127.46 (Cq), 126.64 (CH), 121.13 (CH), 115.87 (CH), 111.06 (CH), 77.16 (Cspiro), 62.39 (CH-4'), 34.74 (C(CH₃)₃), 29.33 (C(CH₃)₃); Anal. Calc. for C₂₆H₂₄ClN₃O.0.05H₂O: C 72.45, H 5.67, N 9.68, Found: C 72.47, H 5.74, N 9.52.

5-bromo-5'-(tert-butyl)-2',4'-diphenyl-2',4'-dihydrospiro[indoline-3,3'-pyrazol]-2-one (2r). Following the general procedure, to a solution of **3e** (0.05 g, 0.18 mmol, 1 eq) in CH₂Cl₂ (2 ml) was added **4d** (0.09 g, 0.43 mmol, 2.5 eq) and triethylamine (0.06 ml, 0.43 mmol, 2.5 eq). Reaction time: 5h30min. The compound was purified by flash chromatography (eluent: EtOAc/*n*-Hexane 1:1) to afford compound **2r** as a white solid (0.03 g, 0.06 mmol, 41.5 %); IR (KBr): 3254 (NH), 1726 (C=O), 1695 (C=N) cm⁻¹; ¹H NMR (300 MHz, CDCl₃) δ 7.69 (s, 1H, NH), 7.48-7.27 (m, 3H, ArH), 7.23 (dd, *J* = 9.0, 2.0 Hz, 2H, ArH), 7.10-7.02 (m, 2H, ArH), 6.86 – 6.80 (m, 3H, ArH), 6.64 (d, *J* = 8.3 Hz, 2H, ArH), 6.27 (d, *J* = 1.9 Hz, 1H, ArH), 4.45 (s, 1H, H-4'), 1.19 (s, 9H, C(CH₃)₃); ¹³C NMR (75 MHz, CDCl₃) δ 177.17 (C=O), 161.68 (C=N), 145.62 (Cq), 139.06 (Cq), 134.71 (Cq), 132.11 (CH), 129.73 (CH), 129.04 (CH), 128.59 (CH), 127.97 (Cq), 121.42 (CH), 116.21 (CH), 115.20 (Cq), 111.45 (CH), 77.36 (Cspiro), 62.63 (CH-4'), 34.91 (C(CH₃)₃), 29.50 (C(CH₃)₃); LC-MS *m/z* calcd for C₂₆H₂₄BrN₃O: 475.1, Found: 476.3 [M⁺H]⁺.

5'-(tert-butyl)-6-chloro-4'-(3-chlorophenyl)-2'-phenyl-2',4'-dihydrospiro[indoline-3,3'-pyrazol]-2-one (2t). Following the general procedure, to a solution of **3h** (0.075 g, 0.26 mmol, 1 eq) in CH₂Cl₂ (2 ml) was added **4d** (0.11 g, 0.52 mmol, 2 eq) and triethylamine (0.11 ml, 0.78 mmol, 3 eq). Reaction time: 18h30min. The compound was purified by flash chromatography (eluent: EtOAc/*n*-Hexane 1:3) and then recrystallized

in diethyl ether to afford compound **2t** as a white solid (0.10 g, 0.23 mmol, 82.7 %); IR (KBr): 3419 (NH), 1720 (C=O), 1616 (C=N) cm^{-1} , ^1H NMR (400 MHz, CDCl_3) δ 8.40 (s, 1H, NH), 7.31 (s, 1H, ArH), 7.28 – 7.20 (m, 2H, ArH), 7.07 (t, $J = 8.0$ Hz, 2H, ArH), 6.90-6.75 (m, 4H, ArH), 6.73 – 6.50 (m, 2H, ArH), 6.18 (s, 1H, ArH), 4.40 (s, 1H, H-4'), 1.19 (s, 9H, $\text{C}(\text{CH}_3)_3$); ^{13}C NMR (101 MHz, CDCl_3) δ 177.60 (C=O), 161.34 (C=N), 145.48 (Cq), 141.42 (Cq), 137.17 (Cq), 135.52 (Cq), 134.81 (Cq), 129.72 (CH), 129.04 (CH), 128.62 (CH), 127.27 (CH), 123.88 (Cq), 122.62 (CH), 121.67 (CH), 116.41 (CH), 111.30 (CH), 76.97 (Cspiro), 61.75 (CH-4'), 34.96 ($\text{C}(\text{CH}_3)_3$), 29.47 ($\text{C}(\text{CH}_3)_3$); Anal. Calcd for $\text{C}_{26}\text{H}_{23}\text{Cl}_2\text{N}_3\text{O}\cdot 0.05\text{H}_2\text{O}$: C 67.25, H 4.99, N 9.05, Found: C 66.61, H 5.14, N 8.82.

5'-(tert-butyl)-2'-(2-chlorophenyl)-4'-phenyl-2',4'-dihydrospiro[indoline-3,3'-pyrazol]-2-one (2u). Following the general procedure, to a solution of **3a** (0.05 g, 0.26 mmol, 1 eq) in CH_2Cl_2 (2 ml) was added **4e** (0.08 g, 0.33 mmol, 1.5 eq) and triethylamine (0.115 mL, 0.083 mmol, 3 eq.). Reaction time: 26h50min. The compound was purified by flash chromatography (eluent: EtOAc/*n*-Hexane 1:4) to afford compound **2u** as a white solid (0.06 g, 0.14 mmol, 61.8 %); IR (KBr): 3419 (NH), 1716 (C=O), 1618 (C=N) cm^{-1} ; ^1H NMR (300 MHz, CDCl_3) δ 7.91 (s, 1H, NH), 7.33 – 7.20 (m, 4H, ArH), 7.18-7.05 (m, 3H, ArH), 6.99 (t, $J = 7.8$ Hz, 1H, ArH), 6.93 (t, $J = 7.8$ Hz, 1H, ArH), 6.67 (d, $J = 7.8$ Hz, 1H, ArH), 6.38 (t, $J = 7.8$ Hz, 1H, ArH), 5.89 (d, $J = 7.6$ Hz, 1H, ArH), 4.40 (s, 1H, H-4'), 1.20 (s, 9H, $\text{C}(\text{CH}_3)_3$); ^{13}C NMR (75 MHz, CDCl_3) δ 178.55 (C=O), 164.14 (C=N), 141.65 (Cq), 140.88 (Cq), 135.54 (Cq), 130.27 (CH), 129.85 (Cq), 129.17 (CH), 128.06 (CH), 127.60 (CH), 127.03 (CH), 125.72 (CH), 124.79 (CH), 123.70 (Cq), 121.52 (CH), 109.49 (CH), 77.95 (Cspiro), 61.79 (CH-4'), 34.93 ($\text{C}(\text{CH}_3)_3$), 29.51 ($\text{C}(\text{CH}_3)_3$); LC-MS m/z calcd for $\text{C}_{26}\text{H}_{23}\text{ClN}_3\text{O}$: 429.2, Found: 430.3 [M^+H] $^+$.

5'-(tert-butyl)-5-chloro-2'-(2-chlorophenyl)-4'-phenyl-2',4'-dihydrospiro[indoline-3,3'-pyrazol]-2-one (2v). Following the general procedure, to a solution of **3b** (0.05 g, 0.02 mmol, 1 eq) in CH_2Cl_2 (2 ml) was added **4e** (0.12 g, 0.41 mmol, 3 eq) and *N,N*-Diisopropylethylamine (0.118 mL, 0.068 mmol, 3 eq.). Reaction time: 21 h. The compound was purified by flash chromatography (eluent: EtOAc/*n*-Hexane 1:4) to afford compound **2v** as a white solid (0.03 g, 0.05 mmol, 27.5 %); IR (KBr): 3383 (NH), 1722 (C=O), 1620 (C=N) cm^{-1} ; ^1H NMR (300 MHz, CDCl_3) δ 8.56 (s, 1H, NH), 7.57 – 7.38 (m, 2H, ArH), 7.33 – 7.22 (m, 3H, ArH), 7.20 – 7.06 (m, 3H, ArH), 6.95 (d,

$J = 5.5$ Hz, 2H, ArH), 6.61 (d, $J = 7.1$ Hz, 1H, ArH), 5.78 (s, 1H, ArH), 4.39 (s, 1H, H-4'), 1.20 (s, 9H, C(CH₃)₃); ¹³C NMR (75 MHz, CDCl₃) δ 178.34 (C=O), 164.16 (C=N), 141.42 (Cq), 139.48 (Cq), 134.91 (Cq), 130.39 (CH), 129.81 (Cq), 129.10 (CH), 128.42 (CH), 127.91 (CH), 127.16 (CH), 126.93 (CH), 126.11 (CH), 125.45 (Cq), 124.95 (CH), 110.47 (CH), 78.18 (Cspiro), 61.93 (CH-4'), 34.94 (C(CH₃)₃), 29.48 (C(CH₃)₃); LC-MS m/z calcd for C₂₆H₂₃Cl₂N₃O: 463.1, Found: 464.3 [M⁺H]⁺.

5'-(tert-butyl)-7-chloro-2'-(2-chlorophenyl)-4'-phenyl-2',4'-dihydrospiro[indoline-3,3'-pyrazol]-2-one (2x). Following the general procedure, to a solution of **3d** (0.07 g, 0.27 mmol, 1 eq) in CH₂Cl₂ (2 ml) was added **4e** (0.11 g, 0.45 mmol, 1.5 eq) and *N,N*-Diisopropylethylamine (0.13 mL, 0.82 mmol, 3 eq.). Reaction time: 22h20min. The compound was purified by flash chromatography (eluent: EtOAc/*n*-Hexane 1:4) to afford compound **2x** as a white solid (0.09 g, 0.2 mmol, 70.8 %); IR (KBr): 3407 (NH), 1712 (C=O), 1620 (C=N) cm⁻¹; ¹H NMR (300 MHz, CDCl₃) δ 7.51 (s, 1H, NH), 7.35 (dd, $J = 8.6, 1.6$ Hz, 1H, ArH), 7.30-7.22 (m, 3H, ArH), 7.20 – 7.10 (m, 3H, ArH), 7.01 – 6.93 (m, 2H, ArH), 6.68 (s, 1H, ArH), 6.40 – 6.29 (m, 1H, ArH), 5.83 (d, $J = 7.6$ Hz, 1H, ArH), 4.42 (s, 1H, H-4'), 1.19 (s, 9H, C(CH₃)₃); ¹³C NMR (75 MHz, CDCl₃) δ 177.63 (C=O), 164.32 (C=N), 141.50 (Cq), 138.70 (Cq), 135.14 (Cq), 130.26 (CH), 130.06 (Cq), 129.14 (CH), 128.24 (CH), 127.19 (CH), 126.22 (CH), 125.94 (CH), 125.53 (CH), 125.18 (Cq), 122.22 (CH), 114.54 (Cq), 78.97 (Cspiro), 61.97 (CH-4'), 34.92 (C(CH₃)₃), 29.46 (C(CH₃)₃); Anal. Calc. for C₂₆H₂₃Cl₂N₃O.0.05H₂O: C 67.24, H 5.00, N 9.05, Found: C 69.62, H 5.12, N 9.19.

4.2. Biological Effects: General Conditions

4.2.1 Cell Culture

HCT-116 cells were grown in McCoy's 5A supplemented with 10% fetal bovine serum (FBS) (Gibco, Thermo Fisher Scientific, Waltham, MA, USA) and 1% penicillin/streptomycin solution (Sigma-Aldrich, St Louis, MO, USA). CCD-18Co cells were grown in DMEM culture medium supplemented with 10% FBS (Gibco), 1% penicillin/streptomycin solution (Sigma-Aldrich), 1% Glutamax (Gibco), 1% Non-Essential Amino Acids Solution (NEAA) (Gibco) and 0.025% TNF- α Human. Cultures were maintained at 37°C in a humidified atmosphere of 5% CO₂. HCT-116 cells were seeded in 96-well plates at 1x10⁴ cells/well for

dose-response curves, cell viability, and cell death assays. Additionally, HCT-116 $p53^{(+/+)}$ cells were seeded in 60-mm dishes at 8×10^5 cells/dish for Western blot analysis, in 24-well plates at 5×10^4 cells/well for evaluation of apoptosis by flow cytometry, and in 6-well plates at 1.5×10^5 cells/well for cell cycle analysis. Finally, CCD-18Co colon fibroblasts cells were seeded in 96-well plates at 4×10^3 cells/well for cell viability assays.

4.2.2. Cell Treatment

Stock solutions of the spiropyrazoline oxindoles were prepared in sterile DMSO. Prior to all treatments, cells were allowed to adhere for 24 h and then exposed to test compounds diluted in culture medium for the mentioned time. To plot dose-response curves, cells were exposed to 0.5-50 μM test compounds. All experiments were performed in parallel with DMSO vehicle control. The final DMSO concentration did not exceed 0.8% (v/v).

4.2.3. Viability assays

Cell viability was assessed 72 h after compound incubation using the CellTiter96® Aqueous Non-Radioactive Cell Proliferation Assay (Promega Corporation, Madison, WI, USA), according to the manufacturer's instructions. This colorimetric assay is based on the bio-reduction of 3-(4,5-dimethylthiazo-2-yl)-5-(3-carboxymethoxyphenyl)-2-(4-sulfophenyl)-2H-tetrazolium inner salt (MTS) to formazan by dehydrogenase enzymes found within metabolically active cells. The amount of water soluble formazan product can be measured by the amount of 490 nm absorbance, correlating with the number of living cells in culture. For this purpose, changes in absorbance were assessed using a GloMax® Multi Detection System (Sunnyvale, CA, USA). For dose-response experiments, best-fit IC_{50} and IC_{80} values from at least three independent experiments were calculated using GraphPad Prism software (version 5.00; San Diego, CA, USA), using the log (inhibitor) vs response (variable slope) function.

4.2.4. Venus-based bimolecular fluorescence complementation (BiFC) assay

To evaluate p53-MDM2 protein-protein interaction, HCT-116 $p53^{(-/-)}$ cells were co-transfected using 1 μg of each BiFC pair plasmid (V1-p53/MDM2-V2) and Lipofectamine 2000 (Invitrogen), following the manufacturer's instructions. Four to six

h after transfection, the medium was replaced with fresh medium, and the compounds in test were added to a final concentration of 5, 10 and 20 μM for additional 20 h. Nutlin-3a at the same concentrations was used as positive control. Equal amounts of vehicle (DMSO) were used as control. Cells were washed twice with Ca^{2+} and Mg^{2+} free PBS (Invitrogen Corp.), treated with accutase and harvested with culture medium. Cell suspensions were centrifuged, supernatants discarded, and cell pellets resuspended in PBS. Fluorescence was measured using a Guava easyCyte™ Flow Cytometer (Merck Millipore) [9,24].

4.2.5. Total protein extraction

HCT-116 $p53^{+/+}$ cells were exposed to the compounds in test at the IC_{50} and $2\times\text{IC}_{50}$ concentration, or vehicle control (DMSO), for 72 h. After that, floating and adherent cells were collected directly in nonyl phenoxypolyethoxylethanol (NP-40) lysis buffer (1% NP-40, 20 mM Tris-HCl pH 7.4, 150 mM NaCl, 5 mM EDTA, 10% Glycerol, 1 mM dithiothreitol (DTT), and 1X proteases and phosphatases inhibitors), followed by sonication and centrifugation at 3200 g for 10 min at 4°C. Total protein extracts were recovered and stored at - 80 °C.

Protein concentration was determined by the colorimetric Bradford method using the Bio-Rad Protein Assay reagent (Bio-Rad), according to the manufacturer's instructions. BSA (Sigma-Aldrich) was used as standard, and absorbance measurements were performed at 595 nm using GloMax-Multi+ Detection System (Promega).

4.2.6. Western blot analysis and densitometric analysis

Protein levels were determined by Western blot analysis. Briefly, total protein extracts were separated on 8 and 14% (w/v) sodium dodecyl sulfate (SDS)-polyacrylamide gel electrophoresis (PAGE) and transferred onto nitrocellulose membranes using the Trans-blot Turbo Transfer System (BioRad). Uniform protein loading and transfer was confirmed by transient staining with 0.2% Ponceau S (Merck, Darmstadt, Germany). Next, nonspecific binding sites were blocked with a 5% milk solution in Tris-buffered saline (TBS) for 1 hour. Membranes were then incubated overnight at 4°C with a mouse monoclonal anti-p53 (Pab-240, sc-99, 1:200) and anti-Mdm2 (SMP-14, sc-965, 1:200), (Santa Cruz Biotechnology, Santa Cruz, CA, USA), or a rabbit polyclonal anti- β -actin (AC-15; 1:8000; Sigma-Aldrich). Membranes were then

washed three times with TBS containing 0.2% Tween 20 (TBS-T), and incubated with anti-rabbit or anti-mouse secondary antibodies conjugated with horseradish peroxidase (Bio-Rad) for 2 h at room temperature. After rinsing three times with TBS-T, the immunoreactive complexes were visualized by chemiluminescence with ImmobilonTM Western (Millipore) or SuperSignal West Femto substrate (Thermo Fisher Scientific, Inc.). Ponceau was used as loading control. Densitometric analysis was performed with the Image Lab software Version 5.1 Beta (Bio-Rad).

4.2.7. Competitive FP binding assay

The binding affinity of spiropyrazoline oxindole was evaluated by a competitive fluorescence polarization-based (FP-based) binding assay, using a recombinant human His-tagged MDM2 protein (residues 1-118) and a FAM tagged p53-based peptide as the fluorescent probe. The design of the fluorescent probe was based upon a previously reported high affinity p53-based peptidomimetic compound (5-FAM- β Ala- β Ala-Phe-Met-Aib-pTyr-(6-Cl-LTrp)-Glu-Ac3c-Leu-Asn-NH₂) [34]. The affinity of this probe compound to MDM2 was determined to be 1.4 ± 0.3 nM by preliminary protein saturation experiments. Mixtures of 5 μ l of the tested compound with different concentrations in DMSO and 120 μ l of preincubated protein/fluorescent probe complex with fixed concentrations in the assay buffer (100mM potassium phosphate, pH 7.5, 100 μ g/ml bovine γ -globulin, 0.02% sodium azide, with 0.01% Triton X-100) were added into assay plates and incubated at room temperature for 30 minutes with gentle shaking. Final concentrations of the protein and fluorescent probe in the competitive assays were 10 and 1 nM, respectively, and final DMSO concentration was 4%. Negative controls containing protein/fluorescent probe complex only (equivalent to 0% inhibition), and positive controls containing free fluorescent probe only (equivalent to 100% inhibition), were included in each assay plate and utilized to calculate inhibition rates. Fluorescence polarization (mP) values were measured using the Infinite M-1000 plate reader (Tecan U.S., Research Triangle Park, NC) in Microfluor 1 96-well, black, round-bottom plates (Thermo Scientific) at an excitation wavelength of 485 nm and an emission wavelength of 530 nm.

4.2.8. General cell death assay

General cell death was evaluated using the lactate dehydrogenase (LDH) Cytotoxicity Detection Kit^{PLUS} (Roche Diagnostics GmbH, Mannheim, Germany),

according to the manufacturer's instructions. The LDH assay measures membrane integrity as a function of the amount of cytoplasmic LDH released into the medium that can be quantified by a coupled enzymatic reaction. In the first step, LDH catalyzes the conversion of lactate to pyruvate via reduction of NAD^+ to NADH. In the second step, diaphorase uses NADH to reduce a tetrazolium salt (INT) to a red formazan product. Thus, the level of formazan is directly proportional to the amount of LDH released, which is indicative of cytotoxicity. Hence, 50 μL of supernatant from treated cells was transferred into a new 96-well plate and incubated with 50 μL of assay substrate for 10 to 30 min, at room temperature, protected from light. Absorbance readings were measured at 490 nm, with 620 nm reference wavelength using a Bio-Rad Model 680 microplate reader. The percentage of LDH release was normalized with DMSO (control).

4.2.9. Apoptosis evaluation

Apoptosis was quantified using the Guava Nexin Reagent kit (Merck Millipore). The Nexin assay uses two distinct dyes, Annexin V to detect phosphatidylserine (PS) on the external membrane of apoptotic cells, and the cell impermeant dye, 7-AAD, as an indicator of membrane structural integrity. For this purpose, HCT-116 $p53^{+/+}$ cells were exposed to: 1) compounds in test at IC_{50} concentration; 2) compounds in test at $2\times\text{IC}_{50}$ concentration, and 3) DMSO (control), for 72 h. After that, the culture medium was collected and cells detached with Accutase. Cells were collected and centrifuged at 500 g for 5 minutes at 4°C . The cell pellet was resuspended in PBS/2% FBS. Subsequently, 50 μL of cell suspension were mixed with 50 μL of Guava Nexin reagent and incubated for 20 minutes, at room temperature in the absence of light. Following the staining procedure, sample acquisition and data analysis of at least 5000 events per sample were performed using the Guava easyCyteTM Flow Cytometer (Merck Millipore) and Nexin software module.

4.2.10. Cell cycle distribution analysis

The effects of compounds on cell cycle progression were determined using a standard propidium iodide staining procedure followed by flow cytometry analysis. Propidium iodide is a fluorescent intercalating agent that has high affinity to nucleic acids. HCT-116 $p53^{+/+}$ cells were treated with the compounds in test at the IC_{50} concentration, or DMSO, for 24 or 48 h. After that, cells were detached with Tryple

reagent and collected by centrifugation at 800 g for 5 min, at 4°C. Cell pellets were resuspended in cold PBS and added an equal volume of 80% ice-cold ethanol (-20°C) drop by drop, while vortexing gently. Samples were stored at -4°C until data acquisition. For cell cycle analysis, cells were centrifuged again at 850g for 5 minutes, at 4°C, and cell pellets were resuspended in 25µg/mL propidium iodide (PI) (Fluka, Sigma-Aldrich) and 50µg/mL RNase A (Sigma-Aldrich) and further incubated for 30 min. Sample acquisition and data analysis were performed using the Guava easyCyte™ Flow Cytometer (Merck Millipore) and Guava analysis software, with the acquisition of at least 10000 events per sample.

4.2.11. Combined Therapy Strategies

5-Fluorouracil was kindly provided by the hospital pharmacy of Hospital Santa Maria in Lisboa. HCT-116 $p53^{+/+}$ cells were treated with compound at IC₁₀, IC₂₀ and IC₅₀ concentrations of **2e** and with the same concentrations of 5-Fluorouracil. The effect of combined treatments on cell growth was analyzed after 72 h incubation, using the MTS assay. Data were analyzed using Excel and GraphPad PRISM software using the following equation, where CDI is coefficient drug interaction: AB is the cell viability ratio of combinatory strategy; A is the cell viability ratio of single agent A; and B is the cell viability ratio of single agent B. Coefficient drug interaction (CDI) is a tool to analyze interaction between drugs allowing distinguishing synergistic, additive and antagonistic effects. For CDI values < 1, drugs have a synergistic effect; for CDI = 1, drugs have an additive effect; and for CDI values > 1, drugs have an antagonistic effect [27,35–44].

$$CDI = \frac{AB}{A \times B}$$

4.3. Statistical analysis

Data were analyzed statistically using the GraphPad software. Differences between means were tested for significance using the Student's t-test (* $p < 0.05$; ** $p < 0.01$; *** $p < 0.001$).

Acknowledgements

This study was supported by Fundação para a Ciência e a Tecnologia, Portugal (FCT) through grant UID/DTP/04138/2013 and fellowship SFRH/BPD/100961/2014 (J. D. A.). M. M. M. Santos would like to acknowledge FCT, “Programa Operacional Potencial Humano” and the European Social Fund for the IF Program (IF/00732/2013). This work was funded in part by iMed.Ulisboa through the Young Investigator’s Project for Collaborative Cross-disciplinary Studies 2015. The authors thank Dr. Shaomeng Wang and Dr. Liu Liu for MDM2 binding testing.

References

- [1] L. Bai, S. Wang, Targeting Apoptosis Pathways for New Cancer Therapeutics, *Annu. Rev. Med.* 65 (2014) 139–155. doi:10.1146/annurev-med-010713-141310.
- [2] L.A. Torre, R.L. Siegel, E.M. Ward, A. Jemal, Global Cancer Incidence and Mortality Rates and Trends--An Update, *Cancer Epidemiol. Biomarkers Prev.* 25 (2016) 16–27. doi:10.1158/1055-9965.EPI-15-0578.
- [3] X.-L. Li, p53 mutations in colorectal cancer- molecular pathogenesis and pharmacological reactivation, *World J. Gastroenterol.* 21 (2015) 84. doi:10.3748/wjg.v21.i1.84.
- [4] A.C. Joerger, A.R. Fersht, The p53 Pathway: Origins, Inactivation in Cancer, and Emerging Therapeutic Approaches, *Annu. Rev. Biochem.* 85 (2016) 375–404. doi:10.1146/annurev-biochem-060815-014710.
- [5] C. Ribeiro, C. Rodrigues, R. Moreira, M. Santos, Chemical Variations on the p53 Reactivation Theme, *Pharmaceuticals.* 9 (2016) 25. doi:10.3390/ph9020025.
- [6] A.K. Gupta, M. Bharadwaj, A. Kumar, R. Mehrotra, Spiro-oxindoles as a Promising Class of Small Molecule Inhibitors of p53–MDM2 Interaction Useful in Targeted Cancer Therapy, *Top. Curr. Chem.* 375 (2017) 3. doi:10.1007/s41061-016-0089-0.
- [7] M.M.M. Santos, Recent advances in the synthesis of biologically active spirooxindoles, *Tetrahedron.* 70 (2014) 9735–9757. doi:10.1016/j.tet.2014.08.005.
- [8] S. Wang, W. Sun, Y. Zhao, D. McEachern, I. Meaux, C. Barriere, J. a Stuckey, J.L. Meagher, L. Bai, L. Liu, C.G. Hoffman-Luca, J. Lu, S. Shangary, S. Yu, D. Bernard, A. Aguilar, O. Dos-Santos, L. Besret, S. Guerif, P. Pannier, D. Gorge-Bernat, L. Debussche, SAR405838: An Optimized Inhibitor of MDM2-p53 Interaction That Induces Complete and Durable Tumor Regression, *Cancer Res.* 74 (2014) 5855–5865.

doi:10.1158/0008-5472.CAN-14-0799.

[9] C.J.A. Ribeiro, J.D. Amaral, C.M.P. Rodrigues, R. Moreira, M.M.M. Santos, Synthesis and evaluation of spiroisoxazoline oxindoles as anticancer agents, *Bioorg. Med. Chem.* 22 (2014) 577–584. doi:10.1016/j.bmc.2013.10.048.

[10] Â. Monteiro, L.M. Gonçalves, M.M.M. Santos, Synthesis of novel spiropyrazoline oxindoles and evaluation of cytotoxicity in cancer cell lines, *Eur. J. Med. Chem.* 79 (2014) 266–272. doi:10.1016/j.ejmech.2014.04.023.

[11] C.J.A. Ribeiro, J.D. Amaral, C.M.P. Rodrigues, R. Moreira, M.M.M. Santos, Spirooxadiazoline oxindoles with promising in vitro antitumor activities, *Med. Chem. Commun.* 7 (2016) 420–425. doi:10.1039/C5MD00450K.

[12] A. Bertamino, M. Soprano, S. Musella, M.R. Rusciano, M. Sala, E. Vernieri, V. Di Sarno, A. Limatola, A. Carotenuto, S. Cosconati, P. Grieco, E. Novellino, M. Illario, P. Campiglia, I. Gomez-Monterrey, Synthesis, in Vitro, and in Cell Studies of a New Series of [Indoline-3,2'-thiazolidine]-Based p53 Modulators, *J. Med. Chem.* 56 (2013) 5407–5421. doi:10.1021/jm400311n.

[13] A. Kumar, G. Gupta, A.K. Bishnoi, R. Saxena, K.S. Saini, R. Konwar, S. Kumar, A. Dwivedi, Design and synthesis of new bioisosteres of spirooxindoles (MI-63/219) as anti-breast cancer agents, *Bioorg. Med. Chem.* 23 (2015) 839–848. doi:10.1016/j.bmc.2014.12.037.

[14] G.M. Ziarani, P. Gholamzadeh, N. Lashgari, Oxindole as starting material in organic synthesis, *Arkivoc.* 2013 (2013) 470. doi:10.3998/ark.5550190.p008.074.

[15] L. Sun, N. Tran, F. Tang, H. App, P. Hirth, G. McMahon, C. Tang, Synthesis and Biological Evaluations of 3-Substituted Indolin-2-ones: A Novel Class of Tyrosine Kinase Inhibitors That Exhibit Selectivity toward Particular Receptor Tyrosine Kinases, *J. Med. Chem.* 41 (1998) 2588–2603. doi:10.1021/jm980123i.

[16] S. Mokhtari, M. Mosaddegh, M. Hamzeloo Moghadam, Z. Soleymani, S. Ghafari, F. Kobarfard, Synthesis and cytotoxic evaluation of novel 3-substituted derivatives of 2-indolinone., *Iran. J. Pharm. Res. IJPR.* 11 (2012) 411–21.

[17] M. Balderamos, H. Ankati, S.K. Akubathini, A. V Patel, S. Kamila, C. Mukherjee, L. Wang, E.R. Biehl, S.R. D'Mello, Synthesis and Structure-Activity Relationship Studies of 3-Substituted Indolin-2-ones as Effective Neuroprotective Agents, *Exp. Biol. Med.* 233 (2008) 1395–1402. doi:10.3181/0805-RM-153.

[18] Y. Zhou, B. Shi, K. Han, Q. Guo, Y. Yang, B. Song, Y. Teng, P. Yu, Design, synthesis and biological evaluation of 3-benzylidene 4-bromo isatin derivatives, *J.*

Chem. Pharm. Res. 5 (2013) 1024–1028.

[19] A. Singh, A.L. Loomer, G.P. Roth, Synthesis of Oxindolyl Pyrazolines and 3-Amino Oxindole Building Blocks via a Nitrile Imine [3 + 2] Cycloaddition Strategy, *Org. Lett.* 14 (2012) 5266–5269. doi:10.1021/ol302425h.

[20] G. Wang, X. Liu, T. Huang, Y. Kuang, L. Lin, X. Feng, Asymmetric Catalytic 1,3-Dipolar Cycloaddition Reaction of Nitrile Imines for the Synthesis of Chiral Spiro-Pyrazoline-Oxindoles, *Org. Lett.* 15 (2013) 76–79. doi:10.1021/ol303097j.

[21] C.J.A. Ribeiro, J.D. Amaral, C.M.P. Rodrigues, R. Moreira, M.M.M. Santos, Synthesis and evaluation of spiroisoxazoline oxindoles as anticancer agents, *Bioorg. Med. Chem.* 22 (2014) 577–584. doi:10.1016/j.bmc.2013.10.048.

[22] S. Wang, W. Sun, Y. Zhao, D. McEachern, I. Meaux, C. Barriere, J.A. Stuckey, J.L. Meagher, L. Bai, L. Liu, C.G. Hoffman-Luca, J. Lu, S. Shangary, S. Yu, D. Bernard, A. Aguilar, O. Dos-Santos, L. Besret, S. Guerif, P. Pannier, D. Gorge-Bernat, L. Debussche, SAR405838: An Optimized Inhibitor of MDM2-p53 Interaction That Induces Complete and Durable Tumor Regression, *Cancer Res.* 74 (2014) 5855–5865. doi:10.1158/0008-5472.CAN-14-0799.

[23] J. Lu, D. McEachern, S. Li, M.J. Ellis, S. Wang, Reactivation of p53 by MDM2 Inhibitor MI-77301 for the Treatment of Endocrine-Resistant Breast Cancer, *Mol. Cancer Ther.* 15 (2016) 2887–2893. doi:10.1158/1535-7163.MCT-16-0028.

[24] J.D. Amaral, F. Herrera, P.M. Rodrigues, P.A. Dionísio, T.F. Outeiro, C.M.P. Rodrigues, Live-cell imaging of p53 interactions using a novel Venus-based bimolecular fluorescence complementation system, *Biochem. Pharmacol.* 85 (2013) 745–752. doi:10.1016/j.bcp.2012.12.009.

[25] L.E. Giono, J.J. Manfredi, The p53 tumor suppressor participates in multiple cell cycle checkpoints, *J. Cell. Physiol.* 209 (2006) 13–20. doi:10.1002/jcp.20689.

[26] K. Somasundaram, Tumor suppressor p53: regulation and function., *Front. Biosci.* 5 (2000) D424-37. <http://www.ncbi.nlm.nih.gov/pubmed/10762600>.

[27] J. Fouquier, M. Guedj, Analysis of drug combinations: current methodological landscape, *Pharmacol. Res. Perspect.* 3 (2015) e00149. doi:10.1002/prp2.149.

[28] T.-C. Chou, Drug Combination Studies and Their Synergy Quantification Using the Chou-Talalay Method, *Cancer Res.* 70 (2010) 440–446. doi:10.1158/0008-5472.CAN-09-1947.

[29] D.B. Longley, D.P. Harkin, P.G. Johnston, 5-Fluorouracil: mechanisms of action and clinical strategies, *Nat. Rev. Cancer.* 3 (2003) 330–338. doi:10.1038/nrc1074.

[30]M. Shakibaei, P. Kraehe, B. Popper, P. Shayan, A. Goel, C. Buhrmann, Curcumin potentiates antitumor activity of 5-fluorouracil in a 3D alginate tumor microenvironment of colorectal cancer, *BMC Cancer*. 15 (2015) 250. doi:10.1186/s12885-015-1291-0.

[31]C.-Y. Zhang, X.-H. Liu, B.-L. Wang, S.-H. Wang, Z.-M. Li, Synthesis and Antifungal Activities of New Pyrazole Derivatives via 1,3-dipolar Cycloaddition Reaction, *Chem. Biol. Drug Des.* 75 (2010) 489–493. doi:10.1111/j.1747-0285.2010.00948.x.

[32]P. Wolkoff, A New Method of Preparing Hydrazone Halides, *Can. J. Chem.* 53 (1975) 1333–1335. doi:10.1139/v75-183.

[33]H. V. Patel, K.A. Vyas, S.P. Pandey, P.S. Fernandes, Facile synthesis of hydrazone halides by reaction of hydrazones with N-halosuccinimide-dimethyl sulfide complex, *Tetrahedron*. 52 (1996) 661–668. doi:10.1016/0040-4020(95)00916-7.

[34]C. García-Echeverría, P. Chène, M.J.J. Blommers, P. Furet, Discovery of Potent Antagonists of the Interaction between Human Double Minute 2 and Tumor Suppressor p53, *J. Med. Chem.* 43 (2000) 3205–3208. doi:10.1021/jm990966p.

[35]D. Wang, Z. Wang, B. Tian, X. Li, S. Li, Y. Tian, Two hour exposure to sodium butyrate sensitizes bladder cancer to anticancer drugs, *Int. J. Urol.* 15 (2008) 435–441. doi:10.1111/j.1442-2042.2008.02025.x.

[36]S. Xu, G. Sun, Y. Shen, W. Peng, H. Wang, W. Wei, Synergistic effect of combining paeonol and cisplatin on apoptotic induction of human hepatoma cell lines, *Acta Pharmacol. Sin.* 28 (2007) 869–878. doi:10.1111/j.1745-7254.2007.00564.x.

[37]J. Tong, G. Xie, J. He, J. Li, F. Pan, H. Liang, Synergistic Antitumor Effect of Dichloroacetate in Combination with 5-Fluorouracil in Colorectal Cancer, *J. Biomed. Biotechnol.* 2011 (2011) 1–7. doi:10.1155/2011/740564.

[38]Y. Jiang, Nicotinamide-mediated inhibition of SIRT1 deacetylase is associated with the viability of cancer cells exposed to antitumor agents and apoptosis, *Oncol. Lett.* 6 (2013) 600–604. doi:10.3892/ol.2013.1400.

[39]S. Torigoe, Y. Ogata, K. Matono, K. Shirouzu, Molecular mechanisms of sequence-dependent antitumor effects of SN-38 and 5-fluorouracil combination therapy against colon cancer cells., *Anticancer Res.* 29 (2009) 2083–9. <http://www.ncbi.nlm.nih.gov/pubmed/19528468>.

[40]C.P. Reynolds, B.J. Maurer, Evaluating Response to Antineoplastic Drug Combinations in Tissue Culture Models, in: *Chemosensitivity*, New Jersey, 2005: pp.

173–184. doi:10.1385/1-59259-869-2:173.

[41]X. Zhou, Y. Zhang, Y. Li, X. Hao, X. Liu, Y. Wang, Azithromycin Synergistically Enhances Anti-Proliferative Activity of Vincristine in Cervical and Gastric Cancer Cells, *Cancers (Basel)*. 4 (2012) 1318–1332. doi:10.3390/cancers4041318.

[42]L. Chen, H.-L. Ye, G. Zhang, W.-M. Yao, X.-Z. Chen, F.-C. Zhang, G. Liang, Autophagy Inhibition Contributes to the Synergistic Interaction between EGCG and Doxorubicin to Kill the Hepatoma Hep3B Cells, *PLoS One*. 9 (2014) e85771. doi:10.1371/journal.pone.0085771.

[43]S.-P. Xu, Antiproliferation and apoptosis induction of paeonol in HepG 2 cells, *World J. Gastroenterol*. 13 (2007) 250. doi:10.3748/wjg.v13.i2.250.

[44]C.C. Uphoff, H.G. Drexler, *Cancer Cell Culture*, Humana Press, Totowa, NJ, 2011. doi:10.1007/978-1-61779-080-5.

- Twenty-three spiropyrazoline oxindoles were synthesized.
- Eight compounds displayed good activities ($IC_{50} < 15 \mu M$) against HCT-116 cells.
- Spiropyrazoline oxindoles induced apoptosis and cell cycle arrest at G0/G1 phase.
- Spiropyrazoline oxindoles were non-cytotoxic to human normal colon fibroblasts.
- A synergistic inhibitory effect was observed with 5-FU.

ACCEPTED MANUSCRIPT